JACS
JOURNAL OF THE AMERICAN CHEMICAL SOCIETY
Article
pubs.acs.org/JACS

Flip-Flop of Steroids in Phospholipid Bilayers: Effects of the Chemical Structure on Transbilayer Diffusion

Giulia Parisio,[†] Maria Maddalena Sperotto,[‡] and Alberta Ferrarini*[,†]

[†]Department of Chemical Sciences, University of Padova, Via Marzolo 1, 35131 Padova, Italy

[‡]Center for Biological Sequence Analysis, Department of Systems Biology, Technical University of Denmark, Kemitorvet, Building 208, 2800 Kgs. Lyngby, Denmark

Supporting Information

ABSTRACT: The transverse motion of molecules from one leaflet to the other of a lipid bilayer, or flip-flop, represents a putative mechanism for their transmembrane transport and may contribute to the asymmetric distribution of components in biomembranes. However, a clear understanding of this process is still missing. The scarce knowledge derives from the difficulty of experimental determination. Because of its slow rate on the molecular time scale, flip-flop is challenging also for computational techniques. Here, we report a study of the passive transbilayer diffusion of steroids, based on a kinetic model derived from the analysis of their free energy surface, as a function of their position and orientation in the bilayer. An implicit membrane description is used, where the anisotropy and the nonuniformity of the bilayer environment are taken into account in terms of the gradients of density, dielectric permittivity, acyl chain order parameters, and lateral pressure. The flip-flop rates are determined by solving the Master Equation that governs the time evolution of the system, with transition rates between free energy minima evaluated according to the Kramers theory. Considering various steroids (cholesterol, lanosterol, ketosterone, 5-cholestene, 25-hydroxycholesterol, and testosterone), we can discuss how differences in molecular shape and polarity affect the pathway and the rate of flip-flop in a liquid crystalline 1,2-dipalmitoyl-*sn*-glycero-3-phosphatidylcholine (DPPC) bilayer, at low steroid concentration. We predict time scales ranging from microseconds to milliseconds, strongly affected by the presence of polar substituents and by their position in the molecular skeleton.

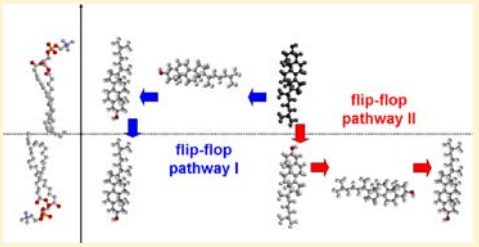

INTRODUCTION

The term flip-flop was first used in 1971, in the pioneering article by Kornberg and McConnell,[1] who referred to it as "the transverse motion of phospholipids" in lipid membranes, also denoted as "inversion" by other authors.[2] The importance of phospholipid flip-flop is related to its role in maintaining a nonuniform molecular distribution between the leaflets of biological membranes.[3] In 1972, Bretscher discovered the asymmetrical organization of phospholipids in erythrocyte membranes and suggested that, to maintain this asymmetry, the transverse diffusion of lipids had to be sufficiently slow.[4] This hypothesis was supported by the earlier experimental studies of Kornberg and McConnell, who had found lifetimes of the order of hours for transbilayer migration in synthetic vesicles.[1] Using NMR spectroscopy, Cullis and de Kruijff inferred a time scale shorter than microseconds for the transverse diffusion of phospholipids in biomembranes and proposed that this process would be facilitated by the formation of transient hexagonal H–II structures.[5] On the other hand Kol et al.,[6] in agreement with a previous hypothesis,[4] suggested that the presence of proteins in membranes, called flippases, would mediate flip-flop and could justify the fast rates. This hypothesis was confirmed by more recent experiments,[7,8] but it was also suggested that fast flip-flop could occur through the formation of transient pores.[9]

Spontaneous transmembrane diffusion, whereas very unlikely for phospholipids, is believed to play a role for cholesterol and fatty acids;[10] pores and proteins would not be required in this case.[11,12] The flip-flop of sterols and fatty acids has been the subject of a number of experimental studies; however, its contribution to lipid trafficking[13,14] and its influence on mechanical and morphological changes in membranes[15−17] are still a matter of debate. As reviewed in refs 10,18, and 19, flip-flop times ranging from a few seconds[20,21] to hours[22−27] have been reported for cholesterol in reconstituted and biological membranes, depending on the experimental method. The study of flip-flop requires the introduction of external fields and molecular probes or of strongly modified lipid analogues. Most assays rely on the transfer of cholesterol from membrane donors to acceptors. The very long time required for the release of cholesterol from lipid bilayers thus limits the detection of fast processes. Recently, a flip-flop time scale of the order of hours was inferred from intervesicle exchange of cholesterol, monitored by time-dependent small-angle neutron scattering.[8] This suggested that proteins could be important also for the translocation of cholesterol in cell membranes. On the other hand, fast interleaflet diffusion of cholesterol, with a residence time shorter than 10 ms, was determined by NMR relaxation experiments on 1-palmitoyl-2-oleoyl-*sn*-glycero-3-phosphatidylcholine (POPC) vesicles.[17] This result was found consistent

Received: April 26, 2012
Published: June 27, 2012

   dx.doi.org/10.1021/ja304007t | *J. Am. Chem. Soc.* 2012, 134, 12198−12208

with a possible role of sterols as mediators of stress relaxation in biological membranes. Also, on the basis of NMR measurements of flip-flop rates for bile acids, fatty acids, and diacylglycerols, the flip-flop of cholesterol was predicted to be very rapid, on the millisecond time scale.[28,29]

Given the difficulty of experimental determination, computational methods represent a useful complement to shed light in this field. However, flip-flop is a slow process on computationally accessible time scales; thus, the observation of translocation events with the available resources remains a challenge. The flip-flop of cholesterol was investigated by a few molecular dynamics (MD) studies, and characteristic times ranging from microseconds to milliseconds were estimated.[30−34] Direct observation of flip-flop was reported for ketosterone in saturated bilayers by all-atom (AA) MD simulations[30] and for cholesterol in unsaturated lipid bilayers by coarse-grained (CG) models.[31] Different pathways were proposed in the two cases, which were mainly ascribed to the different preferential alignment of the steroids near the bilayer midplane in the two lipid systems. However, quantitative rate evaluation and mechanistic hypotheses were precluded by the limited number of events that could be sampled in the course of standard MD simulations. In a recent work, the flip-flop rate of cholesterol was determined on the basis of the potential of mean force (PMF) obtained from umbrella sampling as a function of the sterol position along the bilayer normal.[32,33] In another study a two-dimensional (2D) PMF surface was obtained, as a function of cholesterol position and tilt angle in the bilayer, and the most probable translocation pathway was determined using the string method.[34]

Here, we present a theoretical study of the flip-flop of steroids in lipid membranes. We have calculated the multidimensional PMF as a function of the position and orientation of the steroids in the bilayer. An implicit membrane model has been used, where the anisotropy and the nonuniformity of the environment are taken into account in terms of the gradients of density, dielectric permittivity, acyl chain order parameters, and lateral pressure across the lipid bilayer.[35] Our approach is based on the assumption that well-defined minima can be identified on the free energy surface, separated by large barriers in correspondence of the saddle points, so that the time evolution of the system can be described in terms of transitions between discrete stable configurations.[36] The analysis of the free energy surface allows us to define a kinetic model and to identify the flip-flop pathway. The flip-flop rate is calculated by solving the Master Equation that governs the transitions between the free energy minima, with transition rates evaluated according to the Kramers theory[37] extended to multidimensional diffusion.[38,39] In this way, the description of flip-flop as an activated process[40,41] is derived quite naturally in terms of the underlying energetic and hydrodynamic parameters.

A major feature of our approach, which makes it different from most of the previous studies, is that it accounts for the coupling between rotational and translational degrees of freedom. Indeed, flip-flop is by nature a roto-translational process, which involves both reorientations and displacements across the bilayer. The analysis of flip-flop in terms of a one-dimensional (1D) free energy profile along the bilayer normal would be justified if molecular rotation occurred on a much shorter time scale, so that the transversal displacement could be identified as the slow coordinate;[42] but in principle, there are no arguments in support of such an assumption. Moreover, in reducing flip-flop to a 1D process, all information on the translocation pathway is lost. On the other hand, retaining the complexity of roto-translational diffusion poses some problems: for atomistic simulations, the generation of a multidimensional free energy surface is a computationally demanding task, and the sampling of trajectories for identifying translocation paths requires special strategies.[34] We could overcome such difficulties thanks to some approximations: the kinetic description of flip-flop and the use of an implicit membrane model, which allows us to obtain the multidimensional PMF of a solute in the lipid bilayer at a very low computational cost.

The implicit membrane model used in this work was validated for cholesterol in a liquid crystalline 1,2-dipalmitoyl-*sn*-glycero-3-phosphatidylcholine (DPPC) bilayer: the theoretical predictions compared very well with experimental data from NMR and neutron scattering measurements, as well as with the results of atomistic MD simulations.[35] The same implicit membrane model was adopted also for analyzing the effect of the chemical structure on the positional and orientational distribution of polarity sensitive dyes and fullerene derivatives, in connection with fluorescence[43] and electron spin resonance (ESR)[44] experiments, respectively. The present study focuses on cholesterol and on the steroids shown in Chart 1, in which either the nature and distribution of polar substituents or the structure of the hydrocarbon backbone are varied. We have investigated how these structural differences influence the rate of transverse diffusion in a symmetric liquid crystalline DPPC bilayer. We have examined the case of low steroid concentration, that is, mixtures where the properties of the

Chart 1. Molecular Structures of the Steroids under Investigation[a]

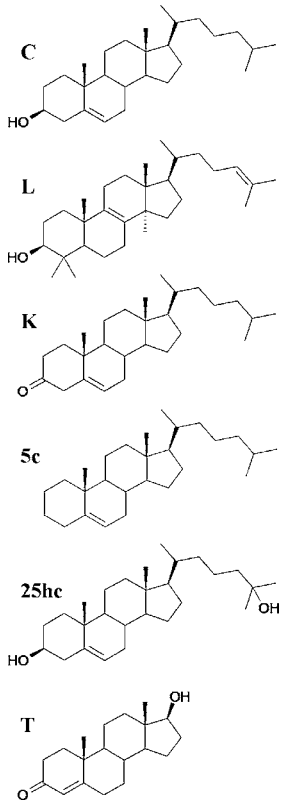

[a]**C** = cholesterol; **L** = lanosterol; **K** = ketosterone; **5c** = 5-cholestene; **25hc** = 25-hydroxycholesterol; **T** = testosterone.

dx.doi.org/10.1021/ja304007t | J. Am. Chem. Soc. 2012, 134, 12198−12208

lipid matrix are substantially unaffected by the presence of the steroid.

In the next section, we will outline the theoretical model and the computational methods. Then, we will report the results of our calculations: we will start with a detailed analysis of the 2D PMF and of the flip-flop process for cholesterol (**C**). Then, the case of lanosterol (**L**), ketosterone (**K**), 5-cholestene (**5c**), 25-hydroxycholesterol (**25hc**), and testosterone (**T**) will be examined. Our results will be discussed in the light of those reported in the literature from other computational studies, though comparison should be taken with some caution, since most of the available data refer to lipid bilayers containing a large amount of steroids.[45,46] In the Conclusion section, we shall summarize what we have learnt on the flip-flop process of steroids in lipid bilayers.

METHODS

Theory. *Free Energy.* Our approach is based on a description of flip-flop as a roto-translational diffusion process in the presence of a PMF determined by steroid−membrane interactions, which depends upon the orientation and the insertion depth of the solute in the lipid bilayer. The model, already presented in detail in ref 35, integrates an atomistic description of the solute and an implicit representation of the lipid bilayer. The PMF experienced by the solute is modeled as the sum of four contributions, related to different types of solute−lipid interactions:[35]

$$U = U_{cav} + U_{el} + U_{disp} + U_{ord} \tag{1}$$

where U_{cav} is the work to create a solute-shaped cavity in the bilayer, U_{disp} accounts for short-range attractive (dispersion) interactions, U_{el} represents the electrostatic free energy of solvation, and U_{ord} introduces the anisotropic interactions with the ordered lipid tails. The nonuniform and anisotropic nature of the membrane environment enters this PMF through the bilayer properties that appear in each contribution: the lateral pressure exerted by the membrane in U_{cav}, the depth-dependent lipid density and dielectric constant in U_{disp} and U_{el}, respectively, and the segmental order parameters of acyl chains in U_{ord}. At low concentration, these properties are assumed to be unaffected by the presence of the solute and can be obtained either from experiments or from MD simulations for the pure lipid bilayer. Therefore, by using this approach, the free energy surface of series of solutes in a specific lipid bilayer is determined at a very low computational cost.

The free energy U in eq 1 is a function of the solute conformational degrees of freedom, of its position across the bilayer, and of its orientation with respect to the bilayer normal (**N**). Based on our previous results for cholesterol,[35] in the present study we ignored the effect of the side chain conformational degrees of freedom on the PMF of the steroids. Calculations were then performed for each steroid with its tail in the all-*trans* conformation (shown in Figure 1 for cholesterol). Given the laboratory frame, $\{X, Y, Z\}$, having its Z axis parallel to **N** ($Z = 0$ at the bilayer midplane), the solute position is specified by the Z coordinate of the origin of the molecular frame, $\{x, y, z\}$. Two angles are needed to define the solute orientation: the polar angle (β) between **N** and the z molecular axis, and the azimuthal angle (γ) that specifies the rotation around this axis. The (canonical) equilibrium positional-orientational distribution function $p(Z, \beta, \gamma)$ of a solute is related to the PMF by the following:

$$p(Z, \beta, \gamma) = \frac{\exp[-U(Z, \beta, \gamma)/k_B T]}{Q} \tag{2a}$$

where Q is the partition function

$$Q = \int \exp[-U(Z, \beta, \gamma)/k_B T] \mathrm{d}Z \sin\beta \mathrm{d}\beta \mathrm{d}\gamma \tag{2b}$$

k_B is the Boltzmann constant and T is the temperature. Reduced distribution functions, which depend upon a smaller number of variables, are obtained from eq 2a by integrating over the unnecessary degrees of freedom; correspondingly, reduced PMFs are defined.[35] So, averaging over the azimuthal angle leads to the 2D free energy surface $u_\gamma(Z, \beta)$, and further averaging over the polar angle yields the 1D free energy profile $u_{\beta,\gamma}(Z)$, as sketched below:

$$\begin{array}{ccccc} p(Z, \beta, \gamma) & \xrightarrow{\text{average over } \gamma} & p_\gamma(Z, \beta) & \xrightarrow{\text{average over } \beta} & p_{\beta,\gamma}(Z) \\ \downarrow & & \downarrow & & \downarrow \\ U(Z, \beta, \gamma) & & u_\gamma(Z, \beta) & & u_{\beta,\gamma}(Z) \end{array} \tag{3}$$

By virtue of the nearly rodlike shape of the derivatives under investigation (Chart 1), the 2D free energy surfaces $u_\gamma(Z, \beta)$ were considered in this work to describe the flip-flop process.

Dynamics. The 2D PMF surface features minima, maxima, and saddle points. The initial (in) and final (fin) states of the flip-flop process are identified with the absolute minima, which for a symmetric bilayer correspond to configurations where the solute is located at the same distance from the bilayer midplane in either leaflet, with antiparallel orientations. If the free energy barriers between the minima are high enough, fast librations in the potential wells can be disregarded and a kinetic description of the diffusion process can be taken.[39] Under these conditions, the equilibrium probability distribution can be approximated by the discrete probabilities of configurations corresponding to the free energy minima, P_j^{eq}, defined as the following:

$$P_j^{eq} = \frac{\exp[-E_j/k_B T]}{\sum_m \exp[-E_m/k_B T]} \tag{4}$$

with the free energy E_j as

$$E_j = u_\gamma(Z_j, \beta_j) + \frac{k_B T}{2} \ln \left| \det \frac{\mathbf{u}_\gamma^{(2)}(Z_j, \beta_j)}{2\pi k_B T} \right| \tag{5}$$

Here, $u_\gamma(Z_j, \beta_j)$ is the 2D free energy and $\mathbf{u}_\gamma^{(2)}(Z_j, \beta_j)$ is the matrix of its second derivatives, both calculated in the jth minimum, at the position and polar angle (Z_j, β_j).

The time evolution of the system is described in terms of transitions between stable states, according to the Master Equation:[47]

$$\frac{\partial P_i(t)}{\partial t} = -\sum_j W_{ij} P_j(t) \tag{6}$$

where W_{ij} is the $j \rightarrow i$ transition rate. In a diffusive process, this is determined by the energetic and frictional properties of the system. We made use of the classical Kramers expression for the rate of escape of a particle from a potential well over a barrier,[37] generalized to diffusion on a multidimensional potential surface;[38,39] in this case, transitions between energy minima involve the crossing of saddle points, which represent the lowest energy barriers.

In determining the rate for the $j \rightarrow i$ transition through the saddle point s of a potential energy surface, a key role is played by the product

Figure 1. Molecular reference frame chosen to define the position and orientation of steroids in the lipid bilayer, shown for cholesterol. The long molecular axis, z, is parallel to the $C_{17} \rightarrow C_3$ direction defined on the steroid rings; the same definition was used for all steroids. The origin of the molecular frame is set in the center of mobility (CM); its position on the steroid backbone depends on the molecular structure.

Table 1. Diagonal Elements of the Roto-Translational Diffusion Tensor Calculated for Cholesterol[a]

D^{T}_{xx} ($cm^2\ s^{-1}$)	D^{T}_{yy} ($cm^2\ s^{-1}$)	D^{T}_{zz} ($cm^2\ s^{-1}$)	D^{R}_{xx} (s^{-1})	D^{R}_{yy} (s^{-1})	D^{R}_{zz} (s^{-1})
1.1×10^{-6}	1.1×10^{-6}	1.3×10^{-6}	1.5×10^{8}	1.5×10^{8}	5.3×10^{8}

[a] D^{T}_{ii} and D^{R}_{ii} represent the diffusion coefficients for translation parallel to and rotation around the i molecular axis, respectively.

$\mathbf{D}_s\mathbf{u}_s^{(2)}$, where $\mathbf{D}_s$ is the roto-translational diffusion tensor and $\mathbf{u}_s^{(2)}$ is the matrix of the second derivatives of the potential energy, both calculated at the saddle point. This product matrix has a single negative eigenvalue, λ_s, whose corresponding eigenvector identifies the crossing direction at the saddle point. The following expression is obtained for the transition rate:[38,39]

$$W_{ij} = (\lambda_s/2\pi)\exp[-(E_s - E_j)/k_B T] \quad (7)$$

where E_j and E_s are the free energies (eq 5) in the jth minimum and at the saddle point, respectively. The description proposed here represents a reasonably good approximation for large to intermediate barrier heights ($E_s - E_j \geq 2k_B T$), in which case paths involving passage far from the saddle points cannot be expected to contribute significantly to the global rate of flip-flop.[39]

The Master Equation, eq 6, was solved assuming that the system is initially in one of the absolute minima, $P_{in}(t = 0) = 1$ and $P_{j\neq in}(t = 0) = 0$. The flip-flop rate constant was then calculated from the time evolution of the probability for the other absolute minimum, $P_{fin}(t)$, according to the following expression:

$$k_{ff}^{-1} = \int_0^\infty \frac{P_{fin}(t) - P_{fin}(\infty)}{-P_{fin}(\infty)} dt \quad (8)$$

where the probability at infinite time is identical to the equilibrium probability, $P_{fin}(\infty) = P_{fin}^{eq}$. In the case of a monoexponential growth with rate constant k_1, the integral in eq 8 is equal to $1/k_1$.

Computational Details. The PMF contributions in eq 1 and the roto-translational diffusion tensor of each derivative in Chart 1 were calculated using an atomistic representation of the steroids. The atomic coordinates of the molecules with their side chain in the all-*trans* conformation were obtained by geometry optimization using density functional theory (DFT), at the B3LYP/6-31 g** level.[48] A common molecular reference frame was chosen for all the compounds, where the long axis, z, was identified with the $C_{17}\rightarrow C_3$ direction defined on the steroid rings (Figure 1). The origin of the molecular frame was set in the center of mobility (CM), where the frictional coupling between translational and rotational motions vanishes.[49] This is the appropriate choice for describing roto-translational diffusion.

Our calculation refer to a symmetric liquid crystalline DPPC bilayer, at the temperature T = 323 K. The properties of this system were parametrized as described in ref 35. The parameters used for solute–membrane interactions are reported in the Supporting Information. Free energy curvatures were evaluated numerically.

The roto-translational diffusion tensors of the steroids were evaluated using a boundary element method for the calculation of the hydrodynamic transport properties of arbitrarily shaped molecules in isotropic and uniform media, with stick boundary conditions.[50] The membrane viscosity was assumed to be similar to that of liquid hydrocarbons.[51] The viscosity value for liquid hexadecane at T = 20 °C (η = 3.3 cP) was used. Very similar results were obtained for all the steroids, with some more difference in the case of testosterone, in view of its smaller aspect ratio. The 6 × 6 roto-translational diffusion tensors are close to diagonal in the molecular frames (Figure 1) and nearly axially symmetric with respect to the z axis, with the z components being larger than the others. Table 1 reports the diagonal elements of the tensor calculated for cholesterol in the molecular frame shown in Figure 1. The complete list of the diagonal elements obtained for all the steroids is reported in the Supporting Information. Experimental values of the translational and rotational diffusion tensors of cholesterol have been reported in the literature, but they usually refer to cholesterol-rich bilayers and therefore may be different from the values in phospholipid membranes with low sterol concentration. From quasi-elastic neutron scattering experiments in 40% mol sterol/DPPC bilayers in the liquid ordered phase, translational diffusion coefficients of the order of 10^{-7} to 10^{-6} $cm^2\ s^{-1}$ were reported for cholesterol.[52,53] For the rotational diffusion tensor, values of the component parallel to the long molecular axis of the order of 10^8 s^{-1} were determined for cholesterol by ^{2}H NMR relaxation experiments in 50% mol sterol/DPPC bilayers[54] and for cholestane in sterol/DPPC bilayers mixtures at various concentrations;[55] for the perpendicular components, there is some ambiguity, since the values derived from experiments depend on the model used to describe the cholesterol dynamics in the ordered environment.

RESULTS AND DISCUSSION

Cholesterol. Figure 2 shows the 2D PMF $u_\gamma(Z, \beta)$ calculated for cholesterol, with its center of mobility (CM in Figure 1) at the position Z along the bilayer normal (**N**) and its long axis (z in Figure 1) forming the angle β with **N**. In the free energy surface, the configurations of interest for our kinetic description of flip-flop can be easily identified: four minima (labeled by numbers) and four saddle points (labeled by

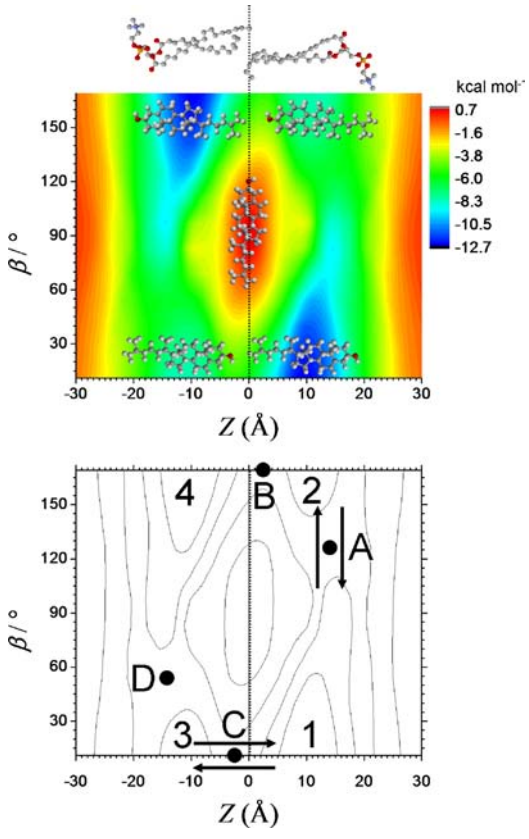

Figure 2. Free energy surface calculated for cholesterol as a function of the position Z of the molecular CM along the bilayer normal (**N**) and of the angle β between **N** and the long molecular axis z. Z = 0 at the bilayer midplane (dashed line). Top: cholesterol molecules are superimposed on the free energy map, in the maximum/minimum energy configurations. DPPC molecules are sketched as a reference. Bottom: absolute and relative minima (**1**–**4**) and saddle points (**A**–**D**) on the free energy map. The arrows indicate the transitions between the free energy minima across the saddle points.

dx.doi.org/10.1021/ja304007t | J. Am. Chem. Soc. 2012, 134, 12198–12208

letters). In all the four minima, cholesterol aligns with its long axis parallel to the bilayer normal and its hydrophobic backbone extending throughout the region of highest lipid density. In the preferred configurations, corresponding to the absolute free energy minima (**1** and **4** in Figure 2), the hydroxyl group interacts at the level of the polar lipid headgroups. These two equivalent states, one in each leaflet of the bilayer, represent the initial and the final state of the flip-flop process. In the other free energy minima (**2** and **3** in Figure 2), cholesterol buries its hydroxyl group in the apolar region of the lipid tails. These configurations are too high in energy to contribute to the equilibrium distribution of cholesterol in membrane but represent intermediate states for the translocation process. These are connected to the stable states (**1** and **4**) through the saddle points (**A**–**D**), which represent the lowest barriers to cross and hence define the preferential routes for the transitions between the minima. The heights of these free energy barriers are collected in Table 2.

Table 2. Free Energy Barriers[a] and Rates[b] for the Transitions in Figure 2, Calculated for C, L, and K

transition		C	L	K
1→**2** through **A**	$E_A - E_1$	10.5	9.2	8.7
	W_{21}	1.6×10^4	9.4×10^4	8.4×10^4
2→**1** through **A**	$E_A - E_2$	4.6	4.4	4.4
	W_{12}	5.5×10^6	1.1×10^7	6.0×10^6
1→**3** through **C**	$E_C - E_1$	11.1	10.2	10.2
	W_{31}	7.3×10^3	2.0×10^4	2.1×10^4
3→**1** through **C**	$E_C - E_3$	5.3	5.5	5.9
	W_{13}	2.6×10^6	2.4×10^6	1.5×10^6

[a] $E_s - E_j$ (eq 5) in k_BT units. [b] W_{ij} (eq 7) in s^{-1} units.

Based on the features of the free energy surface, a four-state kinetic model can be set up. For each transition, the direction of preferential barrier crossing and the transition rate constant are determined by considering simultaneously the roto-translational diffusion tensor and the curvatures of the free energy surface at the saddle point, according to the generalized Kramers theory. The rates of all transitions in Figure 2 are collected in Table 2. It is worth stressing that barrier crossing may occur in a direction different from that of the steepest energy change if motion along another direction encounters lower frictional resistance. In the present case, the transitions through **A** and **D** turn out to have an essentially rotational character, since they mainly involve the upside-down reorientation of cholesterol, while the transition through **B** and **C** are purely translational, since they take the molecule from one leaflet to the other without significantly changing its orientation. Thus, two distinct pathways for the transmembrane translocation of cholesterol can be suggested, which are sketched in Figure 3. Reorientation takes place before translation across the bilayer midplane in the first pathway (I) and after translation in the second (II). This picture excludes the simultaneous reorientation and translation of the molecule, since the direct transfer from **1** to **4**, crossing the free energy maximum, would take place on a very long time scale, which is of the order of seconds.

Starting from the initial condition where cholesterol is found in its preferred configuration in one of the two leaflets, ($P_1(0) = 1$ and $P_2(0) = P_3(0) = P_4(0) = 0$), the time evolution toward the equilibrium distribution ($P_1^{eq} = P_4^{eq} \sim 0.5$; and $P_2^{eq} = P_3^{eq} \sim 0$) is obtained by solving the Master Equation eq 6. A nearly

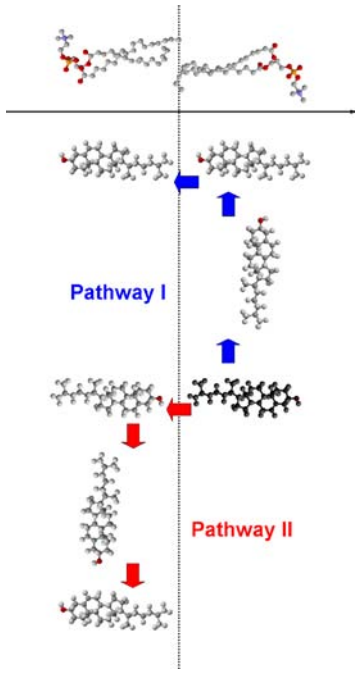

Figure 3. Flip-flop pathways that emerge from our analysis for cholesterol. The dashed line and the black arrow indicate the bilayer midplane and the bilayer normal, respectively. DPPC molecules are sketched as a reference. With reference to Figure 2, the stable state **4** can be reached from the stable state **1**: (I) by crossing the saddle point **A** (**1**→**2**) and then **B** (**2**→**4**); (II) by crossing **C** (**1**→**3**) and then **D** (**3**→**4**).

monoexponential growth of the probability P_4 is found, and a flip-flop rate constant, defined by eq 8, $k_{ff} = 2.0 \times 10^4$ s^{-1} is obtained (Table 3). By comparing the transition rates in Table 2, the reorientation of cholesterol can be identified with the rate determining step of pathway I, while the rate of pathway II is found to be limited by the translation of the molecule through the bilayer midplane. Of the two competing pathways, I is found to be faster than II, and the rate of the global flip-flop process is found to be close to that of the reorientational transition **1**→**2** through **A**.

Table 3. Flip-Flop Rate Constant, k_{ff}, Calculated for the Steroids in Chart 1

	C	L	K	5c	25hc	T
k_{ff} (10^4 s^{-1})	2.0	6.6	6.5	170	11	0.21

The energetic cost associated to the rate-limiting transitions is essentially due to the weakening of electrostatic interactions when cholesterol moves away from the polar region of the bilayer. To check the sensitivity of the result to the parametrization of electrostatic interactions, we repeated our calculations with a set of different atomic charges, and we verified that neither the mechanistic description of the flip-flop process nor its predicted time scale was changed (see the Supporting Information).

There is a general agreement in the literature on the preferred configuration of cholesterol, analogous to that found in our study, although there are some differences in the features of the calculated free energy surfaces. The angular dependence of the free energy surface of cholesterol obtained in ref 32, from orientational sampling during position-restrained simulations in

dx.doi.org/10.1021/ja304007t | J. Am. Chem. Soc. 2012, 134, 12198–12208

a 1:32 sterol/DPPC bilayer at 323 K, is in line with our results: the free energy is found to increase as cholesterol moves from parallel to perpendicular to the bilayer normal, even if variations seem to be less pronounced than in our case. The approach proposed in ref 32 to study flip-flop relies on a 1D treatment of the translocation process and hence cannot provide information on the flip-flop pathway. A flip-flop rate constant in the range 1.2×10^4 to 6.6×10^5 s^{-1} was estimated,[32,33] which is of the same order of magnitude of our prediction; however, a direct comparison is difficult due to the different description of the process. In another recent MD investigation of cholesterol flip-flop in a 1:49 sterol/DPPC bilayer at 323 K, 2D umbrella sampling simulations were performed, and the string method was used to identify the most probable flip-flop path.[34] A flip-flop rate constant in the range 1.2×10^3 to 1.2×10^4 s^{-1} was obtained, which again is of the same order of magnitude of our estimate. However, at variance with our study, cholesterol was found to undergo simultaneous translation and rotation, through a configuration in which it lies at the bilayer midplane, with its long axis perpendicular to the normal. In ref 34, such a configuration corresponds to the saddle point along the most probable flip-flop path, while in Figure 2, as well as in ref 32, it corresponds to a free energy maximum, far apart from the translocation path. This difference might reflect the sensitivity of the orientational preferences of cholesterol to the parametrization of its interactions with the lipid acyl chains. This was recently pointed out, and a modification of the force field used in ref 34 was then proposed by some of the same authors.[56]

Lanosterol and Ketosterone. Lanosterol differs from cholesterol for the presence of three additional methyl substituents on the steroid rings, and ketosterone for the replacement of the hydroxyl headgroup of cholesterol with a carbonyl. For these two derivatives, we have obtained free energy surfaces similar to that of cholesterol, although with some differences in the heights of the free energy barriers, which in most cases, do not exceed k_BT (see Table 2 and the Supporting Information).

To enable an easy comparison between our results and the data reported in the literature, in Figure 4, we show the water-to-membrane transfer free energy profile $u_{\beta,\gamma}(Z)$ and the related equilibrium distribution function, $p_{\beta,\gamma}(Z)$, where Z represents the position of the steroid oxygen atom along the bilayer normal. For all three steroids, we predict high affinity for the lipid bilayer, which increases on going from **L** to **K**, through **C**. The slightly lower stabilization of **L**, compared to **C**, can be mainly ascribed to the fact that the additional methyl groups screen the highly polarizable carbon rings of **L** from contact with the polarizable acyl chain environment. For **K**, the weaker polarity of the carbonyl headgroup lowers the energetic cost associated with its insertion in the apolar region of the bilayer, compared to the hydroxyl group of **C**.

Given the similarity of the free energy surfaces, the same pathways sketched for **C** in Figure 3 can be proposed also for **L** and **K**. To highlight the differences between the three systems, in Figure 5, we show the sections of the free energy surfaces of the steroids at Z = 14 Å and at $\beta = 0°$, which are close to the transition paths for the **1**→**2** reorientation and for the **1**→**3** translation, respectively. For both **L** and **K**, we can see some lowering of the free energy barriers that determine the rates of pathways I and II. This decrease can be traced back to the change of dispersion and electrostatic interactions, for **L** and **K**, respectively, as already discussed in relation to Figure 4. The

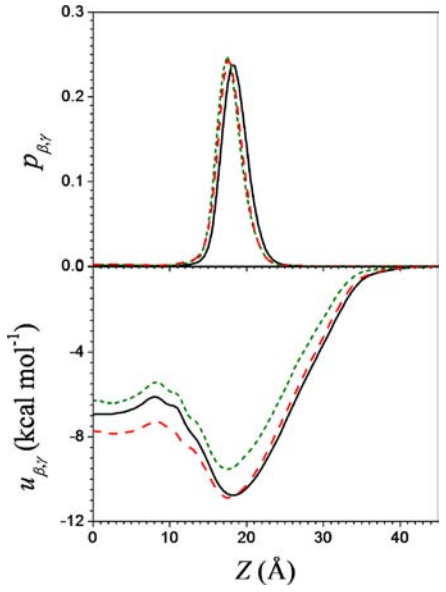

Figure 4. Transfer free energy (bottom) and position distribution (top) calculated for **C** (black solid), **L** (green dotted), and **K** (red dashed) as a function of the position Z of the oxygen atom of the steroid headgroup along the bilayer normal. Z = 0 at the bilayer midplane. Given the symmetry of the bilayer, only one-half of the profile is shown.

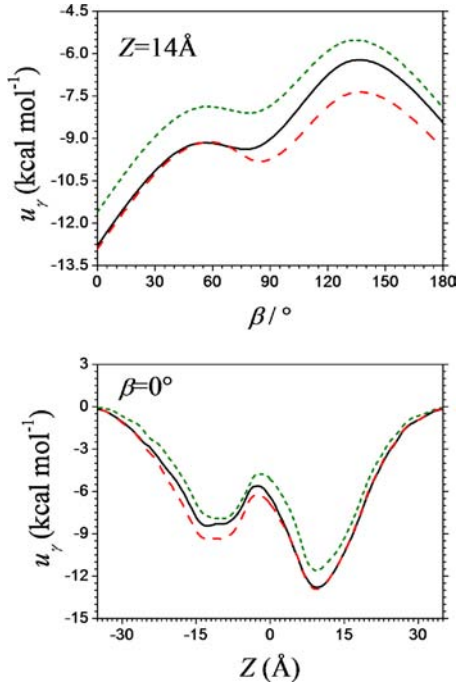

Figure 5. Sections of the free energy surface calculated for **C** (black solid), **L** (green dotted), and **K** (red dashed) close to the paths for the **1** ⇄ **2** reorientation (Z = 14 Å, top) and for the **1** ⇄ **3** translation (β = 0°, bottom).

decrease in the heights of these free energy barriers translates into an increase of the corresponding rate constants (see Table 2). From solution of the kinetic equations, we obtain similar flip-flop rate constants, $k_{ff} = 6.6 \times 10^4$ s^{-1} for **L** and $k_{ff} = 6.5 \times 10^4$ s^{-1} for **K** (Table 3), about three times higher than that for **C**.

dx.doi.org/10.1021/ja304007t | J. Am. Chem. Soc. 2012, 134, 12198−12208

Lanosterol in liquid crystalline 1,2-dimyristoyl-*sn*-glycero-3-phosphatidylcholine (DMPC) at 308 K, in a 1:8 sterol/phospholipid mixture, was studied by MD simulations.[57] As in our calculations, only small differences from analogous simulations for cholesterol were evidenced, and lanosterol was found to reside, on the average, about 1 Å deeper than cholesterol (Figure 4). Moreover, direct observation highlighted larger reorientational mobility of lanosterol, which could easily assume an orientation parallel to the bilayer surface. This is in line with the lower free energy barriers for the reorientation of **L** compared to **C**, obtained from our calculations (Figure 5 and Table 2). More striking differences between the two sterols were observed at higher concentrations where, in agreement with experiment, lanosterol was found to be unable to produce the same ordering and condensing effects as cholesterol.[58]

Miao and co-workers determined lipid−cholesterol and lipid−lanosterol interaction parameters, to reproduce the DPPC/cholesterol phase diagram and the lipid acyl chain order parameters, derived from NMR data, as a function of the sterol concentration.[59] They estimated an interaction strength about 0.14 kcal mol^{-1} higher for cholesterol than for lanosterol; considering the average number of nearest-neighbor lipid molecules interacting with each sterol,[60] a difference in cohesion energy close to 1 kcal mol^{-1} can be estimated, which is comparable with the difference between the free energy minima shown in Figure 4 for the two sterols. Though modest, this amount was found to be sufficient to yield significant effects in the topology of the phase diagram;[59] in particular, the coexistence between the liquid disordered and liquid ordered phases was found for cholesterol, but not for lanosterol, in agreement with experiments.

The behavior of ketosterone was compared with that of cholesterol in MD simulations of 1:4 sterol/DPPC mixtures at 323 K.[30] The ketone group of ketosterone was found to reside slightly deeper than the hydroxyl group of cholesterol, in analogy with the results of our calculations, shown in Figure 4. For ketosterone, two successful flip-flop events were observed in a 200 ns trajectory, from which a time scale of the order of microseconds was estimated for the translocation process. Ketosterone was found to tilt and then to turn upside-down, before moving from one leaflet to the other, in a pathway that closely resembles I in Figure 3. In the same study, a considerably longer time scale was hypothesized for the flip-flop of cholesterol, since no successful events were observed during a 100 ns long simulation. According to our calculations the flip-flop of **K** and **C** takes place with the same dominant pathway (I in Figure 3) and on a time scale that is about three times longer for **C** than for **K**. Our results are not strictly comparable with those reported in ref 30, since in that case, the considerable steroid concentration might affect the bilayer properties. However, the underlying reason of the different behavior of ketosterone and cholesterol, that is, the reduced polarity of the ketone compared to the hydroxyl group, is likely to be general enough to produce effects scarcely dependent on the specific features of the bilayer.

5-Cholestene and 25-Hydroxycholesterol. To further explore the effect of modifying the charge distribution on the translocation rate, we considered two derivatives, obtained from cholesterol either by removing its hydroxyl group (**5c**) or by adding a second hydroxyl group near the end of its side chain (**25hc**). Figure 6, shows the free energy surface calculated for **5c** and **25hc**: there is no strong preference for the head or tail

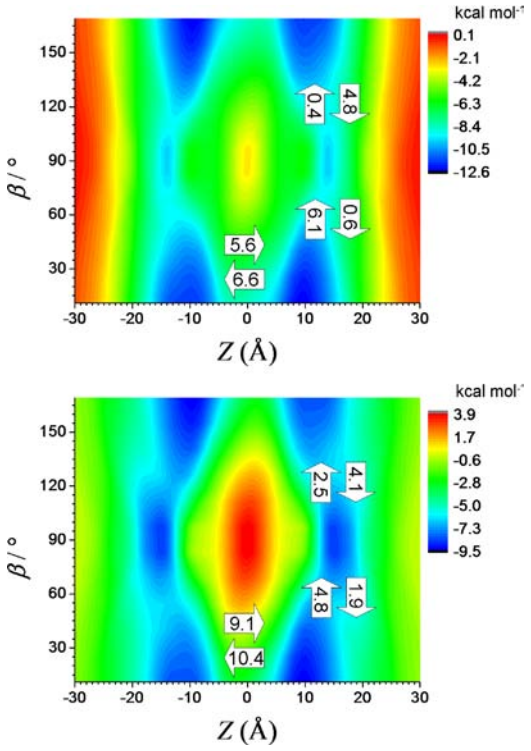

Figure 6. Free energy surface calculated for **5c** (top) and **25hc** (bottom) as a function of the position Z of the molecular CM along the bilayer normal (**N**) and of the angle β between **N** and the long molecular axis z. $Z = 0$ at the bilayer midplane. The arrows indicate the transitions between the free energy minima across the saddle points, and the value on each arrow gives the height of the corresponding free energy barrier (in k_BT units).

of the molecule pointing toward water, and this can be easily understood considering either the absence of a strong dipole or the presence of two polar groups at opposite ends in the molecules. We can see in Figure 6 that, despite the different charge distribution, the preferred position of **5c** and **25hc** remains similar to that of cholesterol: dispersion interactions confine the molecules in the region of highest lipid density, and the depth of the free energy minimum is unchanged for **5c**, while it is reduced by the presence of the additional polar group in **25hc**. On the contrary, we can notice some differences in the orientational preferences: an intermediate minimum appears along the reorientational path between sites **1** and **2**, corresponding to the perpendicular orientation of the steroids at the hydrophobic/hydrophilic interface. For **25hc**, the depth of this minimum is close to that of the minima for the parallel and antiparallel orientation, due to favorable electrostatic interactions of both hydroxyl groups with the polar region of the bilayer. A more complex distribution for **25hc** with respect to cholesterol was found also by MD simulations,[61] where however, unsaturated sterol-rich lipid bilayers were considered.

Since for **5c** and **25hc** the upright and upside-down orientations in a leaflet (sites **1** and **2** in one leaflet, **3** and **4** in the other) are nearly equivalent, we need to define what we mean by flip-flop in these cases. For the ease of comparison with cholesterol, we will still indicate by the term flip-flop the process leading from site **1** to site **4**. Given the shape of the free energy landscapes in Figure 6, a six-site model was adopted for both **5c** and **25hc**, where in addition to the four minima in Figure 2, the two intermediate minima along the reorientational

dx.doi.org/10.1021/ja304007t | J. Am. Chem. Soc. 2012, 134, 12198−12208

paths **1**→**2** and **3**→**4** are included.[62] In both cases, the process can occur through pathways analogous to those denoted as I and II in Figure 3. For **5c**, similar rates are calculated for all transitions exiting from sites **1**−**4**, leading to comparable contributions of the two pathways to the flip-flop process; by virtue of the lower free energy barriers, a flip-flop rate two orders of magnitude higher than that for cholesterol is obtained, k_{ff} = 1.7 × 10^6 s^{-1}. In the case of **25hc**, for both pathways, the rate-determining step is represented by translation through the bilayer midplane, and I is preferred over II because of the slightly lower barrier; the estimated flip-flop rate constant, k_{ff} = 1.1 × 10^5 s^{-1} is five times higher than that for cholesterol.

The effect of the polar group removal or addition on the free energy barriers for **5c** and **25hc** is clearly illustrated by the free energy sections at the fixed orientation β = 0° and at the fixed position Z = 14 Å in Figure 7. We can see that, for both

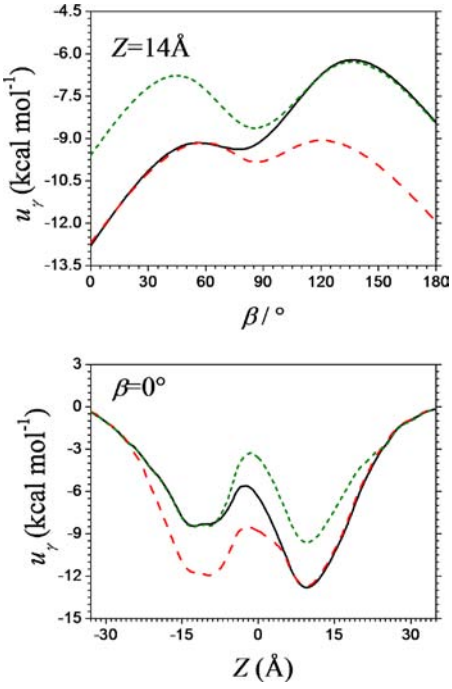

Figure 7. Sections of the free energy surface calculated for **C** (black solid), **5c** (red dashed), and **25hc** (green dotted) close to the paths for the **1** ⇄ **2** reorientation (Z = 14 Å, top) and for the **1** ⇄ **3** translation (β = 0°, bottom).

molecules, the profiles are roughly symmetric and the free energy calculated for **5c** is always lower than that for **25hc**. Comparison with the profiles obtained for cholesterol highlights the role of electrostatic interactions: due to the lack of the polar headgroup, insertion of the steroid head in the bilayer interior is stabilized in the case of **5c**, whereas the presence of the polar side chain end disfavors insertion of the tail of **25hc**. The minima calculated for **5c** and **25hc** are nearly isoenergetic with sites **1** and **2** of cholesterol, respectively.

Testosterone. Compared with **25hc**, testosterone lacks the alkyl tail and has its second polar substituent closer to the rigid core. The absence of the tail has the effect of lowering the affinity of **T** for the lipid bilayer, due to weaker dispersion interactions. Moreover, as a consequence of a shorter distance between the polar ends, the free energy surface of **T** exhibits higher values for configurations in which the hormone is close to the middle of the bilayer and a weaker orientational dependence (Figure 8). The effect of the alkyl tail on the

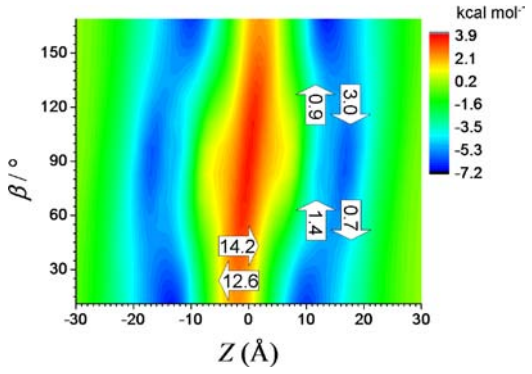

Figure 8. Free energy surface calculated for **T** as a function of the position Z of the molecular CM along the bilayer normal (**N**) and of the angle β between **N** and the long molecular axis z. Z = 0 at the bilayer midplane. The arrows indicate the transitions between the free energy minima across the saddle points, and the value on each arrow gives the height of the corresponding free energy barrier (in k_BT units).

orientational preferences of steroids was investigated by ESR and NMR experiments on nitroxide labeled androstanol and cholesterol analogues in egg yolk phosphatidylcholine at 45 °C: coexistence of the orientations parallel and antiparallel to the bilayer normal was demonstrated for the former, whereas for the latter, a single orientation was evidenced.[63]

As for **5c** and **25hc**, a six-site kinetic model was used for testosterone.[62] In analogy with **25hc**, crossing of the bilayer midplane turns out to be the rate-determining step. Rapid interconversion between the parallel, perpendicular, and antiparallel orientations with respect to the bilayer normal is predicted, in agreement with NMR observations on the androstanol derivative.[63] A flip-flop rate, k_{ff} = 2.1 × 10^3 s^{-1}, about 50 times lower than that predicted for **25hc** is obtained, due to the higher barrier. The section of the free energy surface calculated for **T** at the fixed orientation β = 0° (Figure 9) describes the relevant barrier to testosterone translocation.

Some years ago, a study of the translocation of testosterone across a lipid bilayer, based on a continuum-solvent model, was reported.[64] Testosterone was found to partition in correspondence of the interface between the polar and apolar region of the membrane, with its long axis parallel to the bilayer normal and the hydroxyl group pointing toward water. This corresponds to

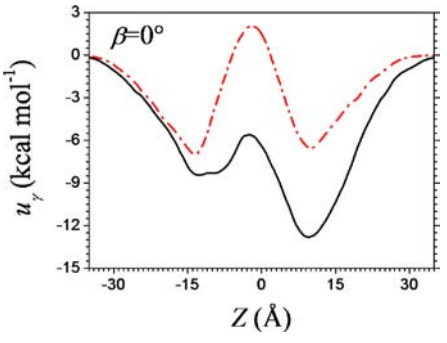

Figure 9. Section of the free energy surface calculated for **C** (black solid) and **T** (red dash-dotted) close to the path for the **1** ⇄ **3** translation (β = 0°).

dx.doi.org/10.1021/ja304007t | J. Am. Chem. Soc. 2012, 134, 12198−12208

the configuration of the absolute minimum in our free energy surface (site **2** in Figure 8). In ref 64, the free energy profiles of testosterone and cholesterol inserting into the bilayer with fixed orientation were reported; the main features of those profiles, as well as the magnitude of wells and barriers, are similar to those appearing in Figure 9, where the sections of the free energy surfaces of **C** and **T** (Figures 2 and 8) at $\beta = 0°$ are shown. In particular, there is agreement on the lower affinity of testosterone for the membrane with respect to cholesterol. The features of the free energy profile of testosterone shown in Figure 9 seem to be quite general for steroid hormones with polar groups at the two ends: in fact, they strongly resemble those of the 1D PMF obtained from atomistic MD simulations of cortisone in a POPC bilayer at 300 K.[65,66] Cortisone was found to partition at the hydrophobic/hydrophilic interface, adopting an orientation perpendicular to the bilayer normal, which was ascribed to favorable electrostatic interactions between its five polar substituents, distributed on its steroid backbone, and the lipid headgroups. In light of these findings, the stabilization that we predict for the perpendicular orientation of testosterone, lower than for the parallel orientation, sounds reasonable. Recently, the behavior of testosterone in a liquid crystalline DMPC bilayer was investigated also by MD simulations using a coarse-grained representation of the lipid bilayer.[67] A broader distribution of the hormone within the bilayer and a tendency for it to align perpendicular to the membrane normal were predicted.

■ CONCLUSION

We have studied the passive flip-flop of steroids in a liquid crystalline DPPC bilayer in the low-concentration regime, and we have explored the effects of chemical modifications on the pathway and time scale of this process. Insights into the effect of chemical substituents on the passive transport of molecular solutes across lipid bilayers can be very important. Whereas there is some general understanding of the relation between the molecular shape and charge distribution of solutes and their affinity for the membrane environment, the effects of structural changes on the dynamical behavior of molecules across lipid bilayers are much less explored. Yet, these changes could have functional implications, relevant for biological processes and pharmacokinetic properties.

Computational methods can be very useful in this context, but appropriate theoretical and/or numerical techniques are needed, due to the characteristic time of the flip-flop process, which is long on the scale accessible by atomistic simulations.[41] We have performed a kinetic analysis of flip-flop, based on the multidimensional Kramers theory for activated processes.[38,39] In this framework, the coupling of rotational and translational degrees of freedom, which is inherent to flip-flop, is taken into account through the free energy and the roto-translational frictional properties of solutes in the bilayer environment. This approach is suitable for slow processes that occur by diffusion through high energetic barriers. Here, 2D free energy surfaces generated by an implicit membrane model have been used,[35] but the method that we propose could be adopted also in the case of free energy surfaces calculated by other methods, for example, by umbrella sampling MD.[32,34] Thanks to the low computational cost of our free energy calculations, we could examine the diffusion behavior of a series of steroids, and we could explore the effect of chemical modifications of the cholesterol backbone.

We have found that steroid flip-flop occurs in general in a nonconcerted way, with rotation and translation taking place as two separated steps. The relative time scales of these transitions, as well as the rate of the global process, vary with the molecular structure, essentially as a consequence of electrostatic effects. However, significant changes in the charge distribution are necessary to produce order of magnitude effects. We have found that molecular size and shape, which are related to nonpolar steroid−membrane interactions, play a minor role, but they can be expected to have a stronger influence at higher sterol concentration or under conditions of tighter lipid packing, for example, in the presence of ordered domains.[15] Although the importance of electrostatic interactions for the molecular distribution in the bilayer is generally recognized, we provide here new insights into their effect on the dynamics. Two flip-flop pathways can be distinguished: (I) first, the steroid rotates and then, it crosses the midplane in the upside-down orientation; (II) first, the steroid moves to the opposite leaflet without substantially changing its orientation, and then, it rotates. Both pathways imply in their first step the embedding of the polar steroid headgroup in the hydrocarbon interior of the bilayer, either by a rotation (I) or by a translation (II) of the molecule. Because of their high free energy barriers, these turn out to be the rate-determining steps of the two pathways, and I is preferred over II, due to the lower barrier of its slow step. According to our calculations, a pathway implying the reorientation of steroids while moving across the bilayer would be unlikely, owing to its high free energy barrier. It is worth stressing that our study refers to a liquid crystalline DPPC bilayer at low steroid concentration, and we expect that the relative importance of different flip-flop paths may change, depending on the bilayer composition and physical state. However, these effects cannot be easily anticipated. The influence of lipid composition, sterol concentration, as well as temperature and pressure on the rate of phospholipid flip-flop has been studied by experiments and simulations. Sum-frequency vibrational spectroscopy experiments on planar-supported bilayers have shown that increasing pressure and decreasing temperature, leading to higher lipid order and packing, result in lower phospholipid flip-flop rates.[68−70] Conversely, increasing rates of phospholipid flip-flop with increasing cholesterol concentration were recently determined by the same technique for bilayers in the solid ordered phase.[71] Neutron scattering experiments have demonstrated the sensitivity of the location and orientation of cholesterol to the bilayer composition and have shown some preference of cholesterol for adopting a perpendicular orientation between the two leaflets of polyunsaturated phospholipid bilayers.[72−74] Recent computer simulations focused on the dependence of the flip-flop rate of cholesterol on the degree of unsaturation of phospholipids[31,32,34] and on cholesterol concentration.[32] A three-order-of-magnitude decrease in the flip-flop rate on going from 0% to 40% of sterol in DPPC was reported. The effect of the bilayer composition on the flip-flop of cholesterol is an important issue, which we intend to address in the future. This can be achieved by our methodology, using a suitable parametrization of the properties that enter the definition of the sterol−bilayer interactions.

In agreement with estimates from MD simulations[30,32,34] and consistently with experimental findings for various systems,[17,28,29] we predict for cholesterol a flip-flop rate on the submillisecond time scale. This does not change significantly for relatively small chemical modifications of the cholesterol

structure that do not involve the distribution of polar groups (like in lanosterol and ketosterone). On the other hand, we predict a significant speed up of flip-flop, with characteristic times even below the microsecond, when the dipole is removed from the headgroup (5-cholestene) or a second dipole is introduced at the end of the tail of cholesterol (25-hydroxycholesterol). On the contrary, the process slows down if the second dipole is attached at the bottom of the sterol core (testosterone). In light of the important role played by electrostatics, it appears conceivable that the presence of charges in phospholipid headgroups can dramatically affect their flip-flop mechanism. The high energetic cost of taking these groups through the apolar region of the bilayer is expected to make spontaneous flip-flop unlikely, so that other competing processes may come into play.[9,12]

■ ASSOCIATED CONTENT

Supporting Information

Parameters used for steroid−bilayer interaction, 2D free energy surfaces and roto-translational diffusion tensors of steroids, results obtained for cholesterol using RESP charges, and further references. This material is available free of charge via the Internet at http://pubs.acs.org.

■ AUTHOR INFORMATION

Corresponding Author

alberta.ferrarini@unipd.it

Notes

The authors declare no competing financial interest.

■ ACKNOWLEDGMENTS

This work was supported by the University of Padova (PRAT 2009). We gratefully acknowledge Prof. Sergio Aragon (San Francisco State University) for the BEST software.

■ REFERENCES

(1) Kornberg, R. D.; McConnell, H. M. *Biochemistry* **1971**, *10*, 1111−1120.
(2) Papahadjopoulos, D.; Ohki, S. *Science* **1969**, *164*, 1075−1077.
(3) de Kruijff, B.; van den Besselaar, A. M. H. P.; Cullis, P. R.; van den Bosch, H.; van Deenen, L. L. M. *Biochim. Biophys. Acta* **1978**, *514*, 1−8.
(4) Bretscher, M. S. *Nat. New Biol.* **1972**, *236*, 11−12.
(5) Cullis, P. R.; de Kruijff, B. *Biochim. Biophys. Acta* **1978**, *507*, 207−218.
(6) Kol, M. A.; de Kruijff, B.; de Kroon, A. I. P. M. *Semin. Cell Dev. Biol.* **2002**, *13*, 163−170.
(7) Contreras, F.-X.; Sánchez-Magraner, L.; Alonso, A.; Goñi, F. M. *FEBS Lett.* **2010**, *584*, 1779−1786.
(8) Garg, S.; Porcar, L.; Woodka, A. C.; Butler, P. D.; Perez-Salas, U. *Biophys. J.* **2011**, *101*, 370−377.
(9) Gurtovenko, A. A.; Anwar, J.; Vattulainen, I. *Chem. Rev.* **2010**, *110*, 6077−6103.
(10) Hamilton, J. A. *Curr. Opin. Lipidol.* **2003**, *14*, 263−271.
(11) Higgins, C. F. *Cell* **1994**, *79*, 393−395.
(12) Marrink, S. J.; de Vries, A. H.; Tieleman, D. P. *Biochim. Biophys. Acta* **2009**, *1788*, 149−168.
(13) Carley, A. N.; Kleinfeld, A. M. *Biochemistry* **2009**, *48*, 10437−10445.
(14) Simard, J. R.; Pillai, B. K.; Hamilton, J. A. *Biochemistry* **2008**, *47*, 9081−9089.
(15) Bacia, K.; Schwille, P.; Kurzchalia, T. *Proc. Natl. Acad. Sci. U.S.A.* **2005**, *102*, 3272−3277.
(16) Ramachandran, S.; Kumar, P. B. S.; Laradji, M. *J. Chem. Phys.* **2008**, *129*, 125104:1−5.
(17) Bruckner, R. J.; Mansy, S. S.; Ricardo, A.; Mahadevan, L.; Szostak, J. W. *Biophys. J.* **2009**, *97*, 3113−3122.
(18) Zachowski, A.; Devaux, P. F. *Experientia* **1990**, *46*, 644−656.
(19) Hermann, A.; Devaux, P. F. *Transmembrane Dynamics of Lipids*; Wiley: Hoboken, NJ, 2012.
(20) Lange, Y.; Dolde, J.; Steck, T. L. *J. Biol. Chem.* **1981**, *256*, 5321−5323.
(21) Steck, T. L.; Ye, L.; Lange, Y. *Biophys. J.* **2002**, *83*, 2118−2125.
(22) Smith, R. J. M.; Green, C. *FEBS Lett.* **1974**, *42*, 108−111.
(23) Kirby, C. J.; Green, C. *Biochem. J.* **1997**, *168*, 575−577.
(24) Lange, Y.; Cohen, C. M.; Poznansky, M. J. *Proc. Natl. Acad. Sci. U.S.A.* **1977**, *74*, 1538−1542.
(25) Backer, J. M.; Dawidowicz, E. A. *Biochim. Biophys. Acta* **1979**, *551*, 260−270.
(26) Bloj, B.; Zilversmit, D. B. *Biochemistry* **1977**, *16*, 3943−3948.
(27) Brasaemble, D. L.; Robertson, A. D.; Ahle, A. D. *J. Lipid Res.* **1988**, *29*, 481−489.
(28) Cabral, D. J.; Small, D. M.; Lilly, H. S.; Hamilton, J. A. *Biochemistry* **1987**, *26*, 1801−1804.
(29) Hamilton, J. A.; Bhamidipati, S.; Kodali, D.; Small, D. M. *J. Biol. Chem.* **1991**, *266*, 1177−1186.
(30) Róg, T.; Stimson, L. M.; Pasenkiewicz-Gierula, M.; Vattulainen, I.; Karttunen, M. *J. Phys. Chem. B* **2008**, *112*, 1946−1952.
(31) Marrink, S. J.; de Vries, A. H.; Harroun, T. A.; Katsaras, J.; Wassall, S. R. *J. Am. Chem. Soc.* **2008**, *130*, 10−11.
(32) Bennett, W. F. D.; MacCallum, J. L.; Hinner, M. J.; Marrink, S. J.; Tieleman, D. P. *J. Am. Chem. Soc.* **2009**, *131*, 12714−12720.
(33) Bennett, W. F. D.; Tieleman, D. P. *J. Lipid Res.* **2012**, *53*, 421−429.
(34) Jo, S.; Rui, J.; Lim, J. B.; Klauda, J. B.; Im, W. *J. Phys. Chem. B* **2010**, *114*, 13342−13348.
(35) Parisio, G.; Ferrarini, A. *J. Chem. Theory Comput.* **2010**, *6*, 2267−2280.
(36) Stocchero, M.; Ferrarini, A.; Moro, G. J.; Dunmur, D. A.; Luckhurst, G. R. *J. Chem. Phys.* **2004**, *121*, 8079−8097.
(37) Kramers, H. A. *Physica* **1940**, *7*, 284−304.
(38) Langer, J. S. *Ann. Phys.* **1969**, *54*, 258−275.
(39) Moro, G. J.; Ferrarini, A.; Polimeno, A.; Nordio, P. L. In *Reactive and Flexible Molecules in Liquids*; Dorfmuller, T., Ed.; Kluwer Academic Publishers: Dordrecht, The Netherlands, 1989; pp 107−139.
(40) Imparato, A.; Shillcock, J. C.; Lipowsky, R. *Eur. Phys. J. E* **2003**, *11*, 21−28.
(41) Martí, J. *J. Phys.: Condens. Matter* **2004**, *16*, 5669−5678.
(42) Neale, C.; Bennett, W. F. D.; Tieleman, D. P.; Pomès, R. *J. Chem. Theory Comput.* **2011**, *7*, 4175−4188.
(43) Parisio, G.; Marini, A.; Biancardi, A.; Ferrarini, A.; Mennucci, B. *J. Phys. Chem. B* **2011**, *115*, 9980−9989.
(44) Bortolus, M.; Parisio, G.; Maniero, A. L.; Ferrarini, A. *Langmuir* **2011**, *27*, 12560−12568.
(45) Róg, T.; Pasenkiewicz-Gierula, M.; Vattulainen, I.; Karttunen, M. *Biochim. Biophys. Acta* **2009**, *1788*, 97−121.
(46) Mannock, D. A.; Lewis, R. N. A. H.; McMullen, T. P. W.; McElhaney, R. N. *Chem. Phys. Lipids* **2010**, *163*, 403−448.
(47) Van Kampen, N. G. *Stochastic Processesin Physics and Chemistry*, 3rd ed.; Elsevier: Amsterdam, The Netherlands, 2007.
(48) Frisch, M. J.; Trucks, G. W.; Schlegel, H. B.; et al. *Gaussian 03*, revision C.02; Gaussian, Inc.: Wallingford, CT, 2004.
(49) Happel, J.; Brenner, H. *Low Reynolds Number Hydrodynamics*; Kluwer Academic Publishers: Dordrecht, The Netherlands, 1965.
(50) Aragon, A. *J. Comput. Chem.* **2004**, *25*, 1191−1205.
(51) Xiang, T.-X.; Anderson, B. D. *Adv. Drug Delivery Rev.* **2006**, *58*, 1357−1378.
(52) Gliss, C.; Randel, O.; Casalta, H.; Sackmann, E.; Zorn, R.; Bayerl, T. *Biophys. J.* **1999**, *77*, 331−340.
(53) Endress, E.; Heller, H.; Casalta, H.; Brown, M. F.; Bayerl, T. M. *Biochemistry* **2002**, *41*, 13078−13086.
(54) Brown, M. F. *Mol. Phys.* **1990**, *71*, 903−908.
(55) Shin, Y. K.; Budil, D. E.; Freed, J. H. *Biophys. J.* **1993**, *65*, 1283−1294.

(56) Lim, J. B.; Rogaski, B.; Klauda, J. B. *J. Phys. Chem. B* **2012**, *116*, 203−210.
(57) Smondyrev, A. M.; Berkowitz, M. L. *Biophys. J.* **2001**, *80*, 1649−1658.
(58) Cournia, Z.; Ullmann, G. M.; Smith, J. C. *J. Phys. Chem. B* **2007**, *111*, 1786−1801.
(59) Miao, L.; Nielsen, M.; Thewalt, J.; Ipsen, J. H.; Bloom, M.; Zuckermann, M. J.; Mouritsen, O. G. *Biophys. J.* **2002**, *82*, 1429−1444.
(60) Huang, J.; Feigenson, G. W. *Biophys. J.* **1999**, *76*, 2142−2157.
(61) Olsen, B. N.; Schlesinger, P. H.; Baker, N. A. *J. Am. Chem. Soc.* **2009**, *131*, 4854−4865.
(62) The description in terms of transition between discrete sites was used also for **5c** and **T**, although in these cases the free energy surface exhibits some shallow minima and low barriers. In fact, in both cases, this assumption does not appreciably affect the flip-flop rate, in view of the time scale separation between the transitions across these low free energy barriers and the rate determining processes.
(63) Morrot, G.; Bureau, J.-F.; Roux, M.; Maurin, L.; Favre, E.; Devaux, P. F. *Biochim. Biophys. Acta* **1987**, *897*, 341−345.
(64) Oren, I.; Fleishman, S. J.; Kessel, A.; Ben-Tal, N. *Biophys. J.* **2004**, *87*, 768−779.
(65) Vijayan, R.; Biggin, P. C. *Biophys. J.* **2008**, *95*, L45−L47.
(66) Strictly speaking, the free energy profile in Figure 9 and the PMF in ref 63 are not directly comparable, since the former is obtained with fixed orientation while an orientational average is hidden in the latter. Actually, for testosterone, we calculated also $u_{\beta,\gamma}$ (Z), by averaging over both angular degrees of freedom according to eq 3, and we found a profile very similar to that shown in Figure 9.
(67) Orsi, M.; Essex, J. W. *Soft Matter* **2010**, *6*, 3797−3808.
(68) Anglin, T. C.; Conboy, J. C. *Biophys. J.* **2008**, *95*, 186−193.
(69) Anglin, T. C.; Conboy, J. C. *Biochemistry* **2009**, *48*, 10220−10234.
(70) Anglin, T. C.; Cooper, M. P.; Li, H.; Chandler, K.; Conboy, J. C. *J. Phys. Chem. B* **2010**, *114*, 1903−1914.
(71) Liu, J.; Brown, K. L.; Conboy, J. C. *Faraday Discuss.* [Online early access]. DOI: 10.1039/C2FD20083J. Published Online: May 10, **2012**. http://pubs.rsc.org/en/content/articlelanding/2012/fd/c2fd20083j
(72) Harroun, T. A.; Katsaras, J.; Wassall, S. R. *Biochemistry* **2006**, *45*, 1227−1233.
(73) Harroun, T. A.; Katsaras, J.; Wassall, S. R. *Biochemistry* **2008**, *47*, 7090−7096.
(74) Kučerka, N.; Marquardt, D.; Harroun, T. A.; Nieh, M.-P.; Wassall, S. R.; Katsaras, J. *J. Am. Chem. Soc.* **2009**, *131*, 16358−16359.